Laser Doppler Anemometry Measurements in Gas-Solid Flows

J. LESINSKI
B. MIZERA-LESINSKA
J. C. FANTON
and
M. I. BOULOS

University of Sherbrooke
Department of Chemical Engineering
Sherbrooke, Québec, J1K 2R1, Canada

Laser Doppler Anemometry (LDA) was used for the simultaneous measurement of the gas and particle velocities in a gas-solid, two-phase flow. The flow configuration consists of an air jet at ambient temperature in which a spherical glass powder of a mean particle diameter of 97.0 or 13.7 μm was injected from one side using a secondary air jet. Both principal and secondary jets were also seeded with talcum powder with a mean particle diameter of about 1 μm which served as a tracer.

The probability density distribution function (PDF) of the LDA output showed two distinct peaks corresponding to the particle and gas velocities. As the particles were accelerated by the flow, the slip velocity between the gas and the particles decreased causing the gap between these two peaks to narrow. The measured mean particle velocity profiles were in agreement with the predictions of a theoretical model.

The objectives of the present investigation was to obtain experimental data on the dependence of the particle trajectories and their mean velocities on the injection conditions in a free jet stream. The principal question, however, was whether such data could be obtained using Laser Doppler Anemometry (LDA). In other words, whether LDA could be effectively used in two-phase flow systems for the simultaneous measurement of the gas and particle velocities? Obviously, the answer to this last question can affect far beyond this particular study and more than justified the effort for this detailed investigation. It should be pointed out that, while LDA has been known for sometime, and the necessary equipments for an LDA system are available on a commercial bases, relatively little attention has been given to its application to other than single-phase, fluid-flow measurements.

SCOPE

The entrainment and acceleration of particles by a fluid stream is the basis of a variety of operations met in the chemical and process industries. It can be associated with unit operations involving only momentum transfer, such as particle feeding in a pneumatic transport line, or the simultaneous transfer of heat, mass and momentum, such as in spray drying, pulverized coal combustion and rocket propulsion.

Recently, with the surge of interest in the development of a heterogeneous, high-temperature plasma processing technology, it became increasingly critical to master this important aspect of particle dynamics. This is due to the fact that in a typical plasma processing unit, whether used for spray coating, spheroidization or chemical reaction, the powder to be treated is pneumatically injected in the plasma jet as it emerges from the plasma-generating device. Whether the treatment would succeed or not then depend on whether the particles were able to penetrate the plasma jet and heat to the required temperature or simply by-passed the hot core of the jet. The strong dependence of the overall efficiency of the powder treatment on the injection conditions was demonstrated by Boulos and Gauvin (1974) using a mathematical model of a plasma jet reactor.

CONCLUSIONS AND SIGNIFICANCE

Laser Doppler Anemometry has been successfully used for the simultaneous measurement of the velocity of the gas and particles as they are injected in a free air jet at ambient temperature.

Measurements are reported for particles with a mean diameter as high as 97.0 μm. The distinction between the velocity of the particles and that of the gas, or more precisely, that of a fine tracer powder of a mean diameter of about 1 μm, was possible through the statistical analysis of the data and the calculation of the probability density distribution function. The results showed that as the particles were entrained by the flow, they attained the velocity of the gas in about 80 to 100 mm from their point of injection. The penetration and spread of the particles in the flow was shown to depend on the mean particle diameter and its size distribution.

The results were in good agreement with the predictions of the stochastic theoretical model of the free jet reactor.

Dr. Lesinski and Mrs. Lesinska are with the Institute of Nuclear Research, 05-400 Swierk/Otwock, Poland.

Mr. Fanton is with the Laboratoire de Spectrométrie Physique de l'Université scientifique et médicale de Grenoble, France.

0001-1541-81-4383-0358-$2.00.

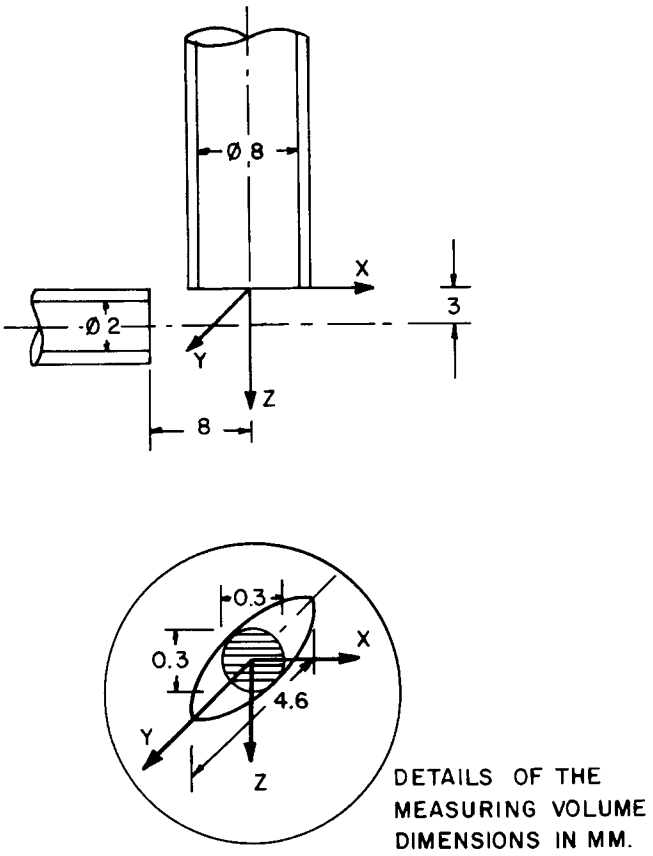

Figure 1. Flow configuration and system of coordinates.

Laser Doppler Anemometry (LDA) is increasingly accepted as a powerful laboratory tool for fluid flow and turbulence measurements over a wide range of conditions. Its principal advantages are the absence of flow disturbing probes and its applicability for measurements under high-temperature conditions such as in a combustion chamber (Self and Whitelaw, 1976) or in a plasma jet (Gouesbet and Trinite, 1977; Lesinski et al., 1979; Vardelle et al., 1979). In the latter case, the gas temperature can be as high as 12,000 K. An excellent review of the state of the art is given by Durst et al. (1976) and Durst (1978).

Recently, LDA has also been suggested for the simultaneous measurement of the gas and particle velocities in gas-solid, two-phase flow. For persons working in the field of pneumatic transport and particle dynamics in general, the simultaneous measurement of these two parameters, the gas and particle velocities, has always been a considerable challenge. On the one hand, gas velocity measurements in the presence of particles are considerably more complicated than that of the gas alone. On the other hand, the measurement of the velocity of the particles was never an easy task whether by high-speed photography (Reddy et al., 1969; Lewis and Gauvin, 1971) or tracer element (Perry and Handley, 1967).

The work of Arundel et al. (1974) is of special interest in this respect, since they were of the first to use LDA to measure particle velocities in pneumatic transport in vertical pipes. The particles used were alumina in the size range 15-200 μm. Their results showed reasonable agreement between the measured centerline slip velocities and those computed from theoretical considerations. Similar measurements were also reported by Stümke and Umbauer (1978) for a gas-solid free flow in a vertical pipe.

The present investigation aims at the study, using LDA, of the entrainment and the acceleration of powders by a free jet as they are pneumatically injected in it from one side. The flow configuration and the system of coordinates used are shown in Figure 1.

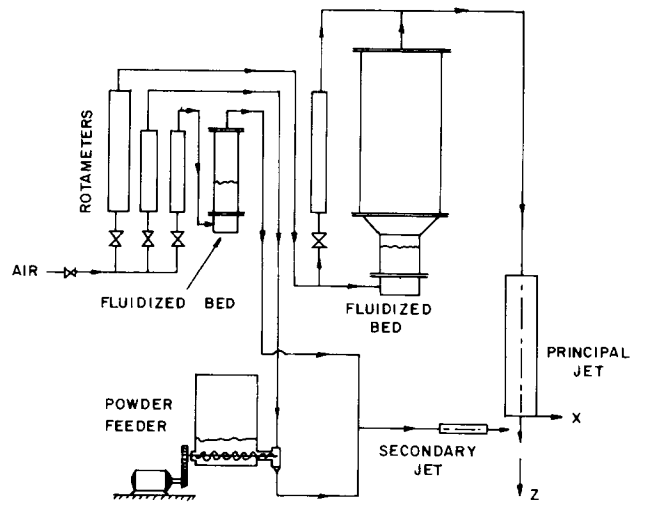

Figure 2. Experimental setup.

EQUIPMENT

The experimental setup is shown in Figure 2. Both the principal and the secondary air jets were at ambient temperature. The principal jet oriented vertically downwards, immerged from an 8-mm I.D. tube, while the secondary jet immerged from a 2-mm diameter tube placed with its centerline 3 mm downstream of the exit of the principal jet directed at 90° to its axis. The distance between the nozzle of the secondary jet and the axis of the main jet was 8 mm.

Measurements were made with two spherical glass powders with a particle density of 2.5 g/cm^3. The particle size distributions were essentially gaussian with a number mean diameter of 97.0 μm and a standard deviation of 10.0 μm for powder A. The number mean diameter and the standard deviation for powder B were 13.7 and 5.5 μm, respectively. The powder feed rates used were about 0.05 g/s for powder A and 0.04 g/s for powder B.

In order to be able to measure the gas velocity, both principal and secondary jets were also seeded with a very fine talcum powder of a particle density of 2.7 g/cm^3 and a number mean particle diameter of about 1 μm. The seeding was achieved as shown in Figure 2, by passing part of each air stream through a fluidized bed of relatively large glass spheres, about 150 μm, to which a small percentage of the talcum powder was added. The powder elutriated uniformly from each bed at a rate which depend on the concentration of the powder in the bed and the superficial velocity of the air. Such a seeding technique was relatively simple and was found to be very satisfactory. In fact, if the superficial air velocity in the fluidized bed was relatively low, the bed could be operated for more than an hour with little change in the elutriation rate.

In order to allow for the seeding of the ambient air entrained by the jets, and to avoid spreading the talcum powder in the lab space, the jets were partially enclosed in a 0.4 × 0.4 m rectangular chamber, 1.0 m long from which the air was eventually evacuated by an exhaust fan. This resulted in the recirculation of the seeded air without affecting the flow field.

The LDA system used was a Thermo Systems Inc. (TSI) counter-type model 1980 with a 35 mW Helium-Neon Laser. The unit was used in the forward scatter mode with its optical axis perpendicular to the X—Z plane. The beam spacing was 50 mm and the focal length of the transmitting and receiving lenses was 247 mm. This gave rise to a measuring volume in the form of an ellipsoid of major and minor axis of 4.6 and 0.32 mm, respectively. The interference fringe spacing was 3.2 μm.

As a particle passed through the measuring volume, it produced a light burst modulated at a frequency in the range of 0.5-40 MHz which was a function of its velocity and the fringe spacing. The photomultiplier signal, after being processed by the signal conditioner and the counter module gave the time

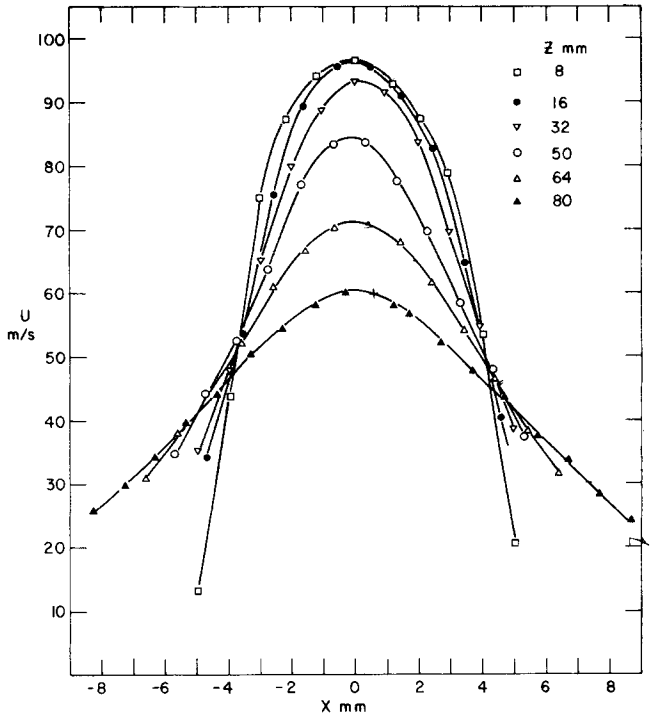

Figure 3. Axial velocity profiles in the absence of glass particles.

required for the particle to traverse a fixed number of fringes (32 in most cases). This information, as it become available at the digital data output of the unit, was transmitted to a Motorola 6800 microprocessor which stored it in its 36 K memory. The unit was programmed for the acquisition of any specified number of data points up to 10,000. Most of the results reported in this study were obtained with a minimum of 5,000 data points.

The number of fringes to be used could be set to 2, 4, 8, 16 or 32. Increasing the number of fringes improved the accuracy of the measurement as well as the spatial resolution. In our case, by using 32 fringes, the measuring volume could be effectively reduced to an ellipsoid with major and minor axis about 3.0 and 0.3 mm, respectively. Another parameter which could influence the results was the setting of the low- and high-pass filters on the signal conditioner. These served to remove the high-frequency noise and signal pedestal, respectively. Because of the relatively low-noise level of the signals, most measurements were made without the low-pass filter. The high-pass filter was set between 0.3 and 3 MHz depending on the doppler frequency to be measured.

At the end of the data acquisition period which could last from a few seconds to one or two minutes, the microprocessor performed a complete statistical data analysis giving the minimum and maximum velocities, the mean velocity, the standard deviation as well as the probability density distribution function (PDF). This was displayed on an oscilloscope screen and was also printed in tabulated form.

It should be noted that the computed mean and standard deviation of the PDF had a physical significance, only if the measurement was that of the gas or particle velocity distribution alone, but not for the simultaneous measurement of these two values. Under such condition, the PDF had two distinct peaks corresponding to the gas and particle velocities. The mean and standard deviation for each could be determined from the oscilloscope display or the tabulated values of the PDF. Since for a symmetrical distribution the mean would coincide with the maximum of the distribution, the velocities corresponding to the respective peaks on the PDF were used as a measure of the mean gas and particle velocities. Based on preliminary results, the mean gas and particle velocity measurements were found to be reproducible to better than ±1.0% over the velocity range between 10 and 120 m/s.

Because the optical setup was relatively elaborate, it was easier to traverse the principal and secondary jets with respect to the LDA system rather than the other way round. This was achieved by fixing the two jets in a rigid configuration mounted on an X—Y—Z traverse with micrometric adjustment to a precision better than 0.1 mm. The same measurements could also be done the other way round (Lesinski et al., 1979), i.e., by fixing the test configuration and moving the LDA. The choice between one arrangement or the other was simply a matter of convenience and the availability of the necessary accessories at that time.

EXPERIMENTAL RESULTS

Measurements were first made of the gas velocity profiles in the absence of glass particles for an exit centerline velocity of the main and secondary jets of 95.0 and 20.0 m/s, respectively. Under such conditions, the total momentum ratio between the two jets ($U_s^2 D_s^2/U_o^2 D_o^2$) was small enough to ensure that the secondary jet had a negligible influence on the trajectory of the principal jet.

Axial velocity profiles at different levels in the flow field are shown in Figure 3. Because of the light seeding of the ambient air compared to the main jet, measurements were restricted to the central region of the flow. This happened to be also the region where most of the glass particles injected into the jet were entrained. Immediately downstream of the exit of the principal jet, the velocity profiles were those of a fully developed turbulent pipe flow. This was rather expected since the principal jet immerged from an 8-mm I.D. tube, 200-mm long. The Reynolds number of the flow was 4.85×10^4. Further downstream, the velocity profile flattened acquiring its typical gaussian shape in the fully developed region of the flow.

Figure 4 gives the variation of the centerline velocity (U_c/U_o) and the intensity of turbulence ($\hat{u}/U_c$) along the axis of the jet. The length of the core region was only about three- to five-nozzle diameters. Beyond this region, the centerline velocity dropped gradually according to the following correlation for $5 < z/D_o < 15$.

$$\frac{U_c}{U_o} = 9.7/[(z/D_o) + 5.3] \qquad (1)$$

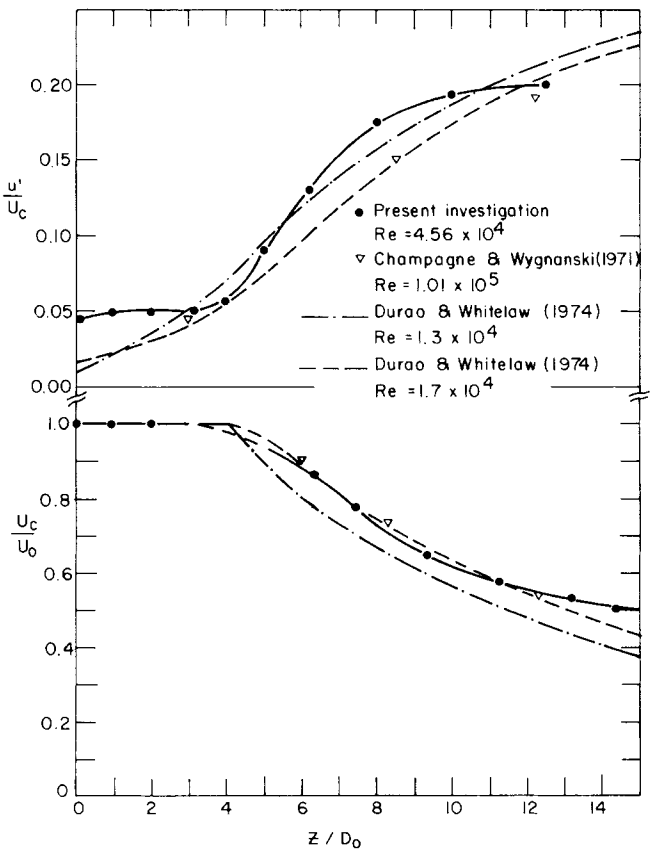

Figure 4. Gas velocity and the intensity of turbulence along the centerline of the principal jet.

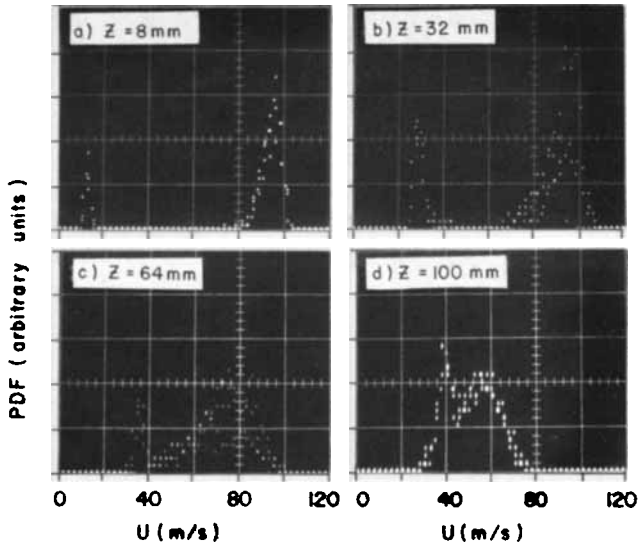

Figure 5. Probability density distribution function in the presence of the 97.0-μm powder, at different levels along the centerline of principal jet.

The relative shortness (Hinze, 1975) of the core region in this case can be attributed to the high level of turbulence in the flow at the exit of the tube ($\dot{u}/U_c \simeq 5\%$). The upper part of Figure 4 shows that the intensity of turbulence along the axis of the flow was almost constant throughout the core region. Beyond this region, it increased systematically to about 20% at $z/D_n = 12$. The present measurements of the mean gas velocity and the intensity of turbulence are in agreement with Champagne and Wygnanski's (1971) hot wire anemometry data and the Durao and Whitelaw's (1974) measurements obtained using LDA for a single free jet.

Further measurements were then made of the velocity in the presence of the glass as well as the tracer talcum powder. Typical oscilloscope displays of the probability density distribution functions obtained with the 97.0-μm powder at z = 8, 32, 64 and 100 mm along the centerline of the principal jet are given in Figure 5. The two peaks distinctly apparent in Figure 5-a correspond to average particle and gas velocities of 13.1 and 95.0 m/s respectively. Their relative height,

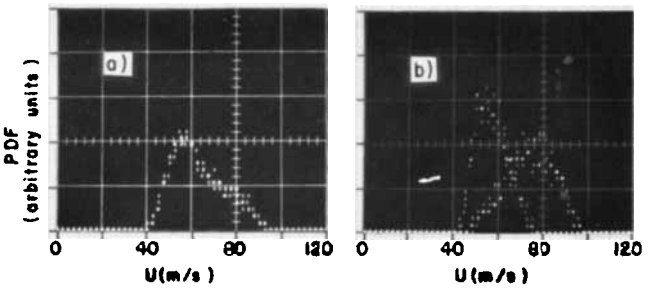

Figure 6. Probability density distribution function in the presence of 13.7-μm powder at z = 64 mm, on the centerline of principal jet.

however, depends on the number of heavy (97.0 μm) and tracer (1 μm) particles counted over the measurement time. As the particles were entrained by the principal jet they were accelerated, while the gas decelerated until the slip velocity between the two became negligible. This is clearly demonstrated by the narrowing of the gap between the two peaks and their eventual merger noted in Figures 5-b, c and d.

It is interesting to point out that even as the two peaks merge, Figure 5-d, they could still be distinguished from each other. This was not always the case as shown in Figure 6-a which was obtained with the 13.7-μm powder, 64 mm downstream of the exit of the principal jet along its centerline. Here, the contribution of the gas and particle velocity distributions to the PDF shown in Figure 6-a could only be determined by separately measuring each of them and superimposing the results on the same oscillogram as shown in Figure 6-b.

Mean particle velocity profiles with the 97.0-μm powder at different levels downstream of the exit of the principal jet are given in Figure 7. The particle injection velocity, V_{pi}, had a gaussian probability density distribution with a mean of 5.0 m/s and a standard deviation of 0.7 m/s. Due to the relatively large diameter and narrow size distribution of the particles (their standard deviation was only 10.0 μm) the particles did not spread over the whole flow field. As a result, some regions of the flow did not contain enough particles for meaningful measurements.

Similar profiles, Figure 8, were obtained with the 13.7-μm powder injected at the same mean velocity as that of the 97.0-μm particles. Due to the smaller inertia of the particles in this case, they penetrated the flow less than the 97.0-μm particles, but were accelerated to higher velocities.

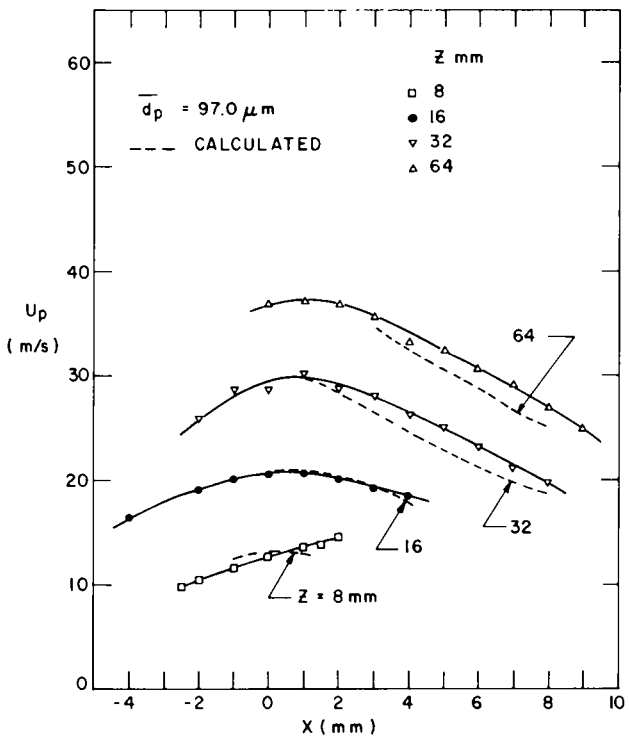

Figure 7. Mean particle velocity profiles for the 97.0-μm powder for a mean injection velocity of 5.0 m/s.

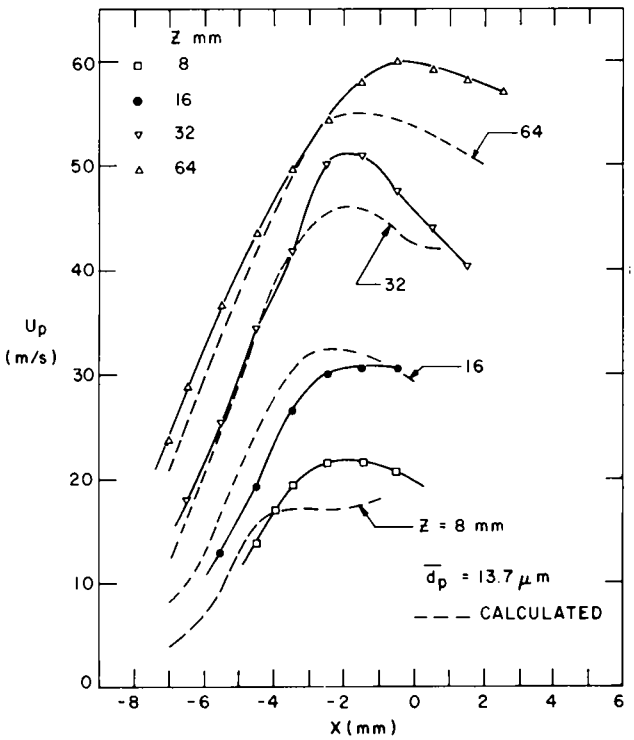

Figure 8. Mean particle velocity profiles for the 13.7-μm powder for a mean injection velocity of 5.0 m/s.

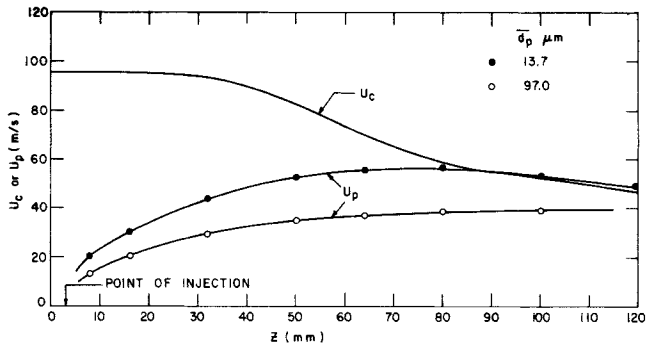

Figure 9. Mean particle velocity along the centerline of the principal jet.

Figure 9 shows the mean axial particle velocities for the 97.0- and 13.7-μm powders along the centerline of the principal jet. Superimposed is also the axial gas velocity, U_c.

The 97.0-μm powder reaches a velocity plateau of about 38 m/s at 80 mm from the point of injection. The 13.7-μm powder reaches its plateau at about the same distance, except that its velocity at this point is close to 56 m/s. Further downstream, the 13.7-μm particles gradually decelerate as the velocity of the gas decreases.

THEORETICAL MODEL

In order to calculate the trajectories and the mean particle velocities in the jet, a theoretical model was developed similar to that of Boulos and Gauvin (1974) and Fiszdon and Lesinski (1975). The model implied the following assumptions:

1. Negligible particle-gas interaction, i.e., the flow field in the free jet, is independent of the presence or absence of the glass particles. This assumption is generally true in gas-solid, two-phase flow system at low loading ratios. Since the loading ratio in our case was less than 1 g solid/100 g gas, it was felt that this assumption was acceptable.

2. Turbulent diffusion had a negligible effect on the particle trajectories. While this is not necessarily true for very small particles, it was justifiable for the relatively large particles used in this investigation which, due to their inertia, are not able to follow the turbulent fluctuations of the flow, Soo (1967) and Richards (1977).

The approach used was to calculate, using the experimentally determined gas velocity profiles in the jet, single-particle trajectories for different size particles with different injection velocities. A statistical analysis of these trajectories was then made to obtain the probability associated with each trajectory, and thus the probability density distribution function for the particle velocities at any point in the flow field.

Single-particle Trajectory Calculations

Single-particle trajectories were calculated by solving a simplified form of the Basset-Boussinesq-Oseen equation after neglecting the history and added mass terms which are known to be important only under very high-acceleration conditions. The equations for the axial and radial particle velocities could then be written as follows for a jet-oriented, vertically downwards.

$$\frac{dU_p}{dt} = (-3/4)\, C_D(U_p - U)\,|U_R|\,(\rho/\rho_p d_p) + g \qquad (2)$$

$$\frac{dV_p}{dt} = (-3/4)\, C_D(V_p - V)\,|U_R|\,(\rho/\rho_p d_p) \qquad (3)$$

where

$$U_R = [(U_p - U)^2 + (V_p - V)^2]^{1/2} \qquad (4)$$

The above equations also implied that the particle density, ρ_p, was much larger than the fluid density, ρ. The drag coefficient,

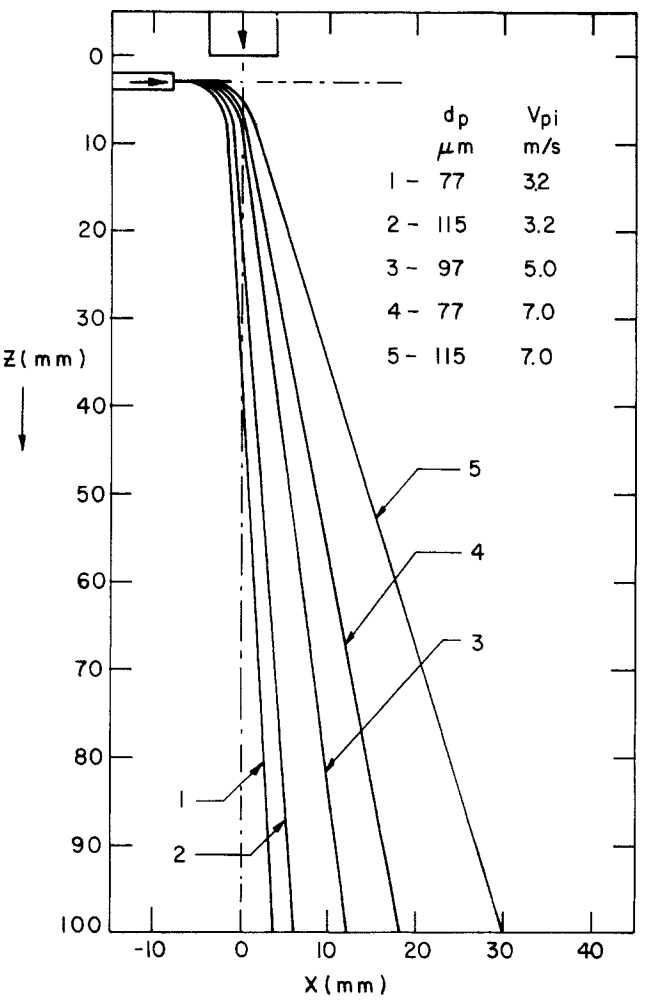

Figure 10. Calculated single-particle trajectories.

C_D, was calculated as function of the Reynolds number ($Re = \rho U_R d_p/\mu$) using the following correlations.

$$C_D = 24/Re \qquad Re < 0.2 \qquad (5)$$

$$C_D = (24/Re)[1 + (3/16)\,Re] \qquad 0.2 \leq Re < 2.0 \qquad (6)$$

$$C_D = (24/Re)[1 + 0.11\,Re^{0.81}] \qquad 2.0 \leq Re < 21.0 \qquad (7)$$

$$C_D = (24/Re)[1 + 0.189\,Re^{0.632}] \qquad 21.0 \leq Re < 200.0 \qquad (8)$$

Eqs. 2 and 3 were solved with appropriate boundary conditions using a Runge-Kutta-Merson subroutine with a variable step size. In all of the computations, the radial gas velocity was assumed to be null, $V = 0$. The axial gas velocity was based on the experimental measurements.

Typical trajectories obtained for different particle diameters, d_p, and injection velocities, V_p°, are shown in Figure 10. Both the diameter and the particle injection velocity significantly influences its trajectory.

Multiparticle Model

The multiparticle model was developed by dividing the particle size distribution of the powder into "m" discrete fractions, d_{pj}, each with a probability P_j, with $j = 1 \ldots m$. It was then assumed that each of these fractions was injected into the jet with "n" different velocities, V_{pi}°, each with a probability P_i, with $i = 1 \ldots n$. Combining these two distributions gives rise to ($n \times m$) different trajectories with a probability, P_{ij}, associated with each of them.

$$P_{ij} = P_i \cdot P_j \tag{9}$$

with P_i and P_j normalized, P_{ij} will also be normalized; i.e., at each level in the jet:

$$\sum_{j=1}^{m} \sum_{i=1}^{n} P_{ij} = 1 \tag{10}$$

The local probability density distribution functions at any point in the jet could then be calculated by taking into account only those trajectories that pass in its neighbourhood (±1.5 mm).

With the particle-size distribution of the powder, and the injection velocity distribution, divided into 20 discreet fractions each, no more than 30 or 40 trajectories passed within ±1.5 mm of any one point in the flow field. While these were sufficient to calculate the mean particle velocity at that point they were too few to determine the PDF of the particle velocity with reasonable accuracy. One should note that in the experimental measurements, the statistical analysis was carried out for some 5,000 to 10,000 particles at any point.

Typical results obtained with the present model for the 97.0- and 13.7-μm powders have been superimposed on Figures 7 and 8. These are in good agreement with the experimental data especially far from the point of injection of the particles. At $z = 8$ mm, the agreement between the model and the experimental data is less satisfactory. This could be due to either the insufficient spatial resolution of the LDA measurements at this level, or the simplifying assumption implied by the model that all the particles were injected at a single point in space ($x = -8$, $z = 3$ mm).

It is interesting to note that the same model could be used to calculate the particle-size distribution in the jet at different levels. Typical results obtained with the 97.0- and the 13.7-μm powders showed an important particle segregation with the largest particles penetrating the deepest in the jet. These model predictions, however, could not be verified since no particle-size measurements were made. This is, however, possible since the pulse generated by the passage of each particle in the field of measurement contains information about its size (Andrews and Seifert, 1972; Durst and Umhauer, 1975; Durst, 1978; Farmer, 1978).

CONCLUSIONS

From the results of the present investigation, it can be concluded that counter-type Laser Doppler Anemometers can be effectively used for the simultaneous measurement of the gas and particle velocities in gas-solid, two-phase flows. Measurements were made with solids of a mean particle diameter as high as 97.0 μm. Talcum powder with a mean particle diameter of 1 μm was used as a tracer for the gas velocity. Mean particle velocity profiles obtained for different spherical glass powders injected in a free air jet were in agreement with the prediction of a proposed theoretical model.

ACKNOWLEDGMENT

The financial support by the National Research Council of Canada and the Ministry of Education of the province of Quebec are gratefully acknowledged. This work was also partially supported by the Department of Energy (Office of Basic Energy Sciences) through contract EE-77-S-02-4320.

NOMENCLATURE

C_D = drag coefficient
d_p = particle diameter, μm
D_o = nozzle diameter of the principal jet, mm
D_s = nozzle diameter of the secondary jet, mm
g = gravitational acceleration, m/s^2
P = probability
Re = Reynolds number, $\rho U_R d_p/\mu$
t = time, s
$\acute{u}$ = root mean square of the axial gas velocity fluctuations, m/s.
U = axial gas velocity, m/s
U_c = jet centerline velocity, m/s
U_o = exit centerline velocity of the principal jet, m/s
U_p = axial particle velocity, m/s
U_R = relative velocity between the particle and the gas, Eq. 4
U_s = exit centerline velocity of the secondary jet, m/s
V = radial gas velocity, m/s
V_p = radial particle velocity, m/s
V_p° = particle injection velocity, m/s
x = distance along the x direction measured from the axis of the principal jet, mm
y = distance along the y direction measured from the axis of the principal jet, mm
z = distance along the z direction measured from the exit of the principal jet, mm

Greek Letters

μ = dynamic viscosity, g/m · s
ρ = fluid density, kg/m^3
ρ_p = particle density, kg/m^3

LITERATURE CITED

Andrews, D. G., and H. S. Seifert, "Investigation of Particle-Size Distribution from the Optical Response of a Laser-Doppler Velocimeter," Stanford University project Squid Report Su-1-PU (1972).

Arundel, P. A., C. A. Hobson, M. J. Lalor, and W. Weston, "Measurements of Individual Alumina Particle Velocities and the Relative Slip of Different-Sized Particles in a Vertical Gas-Solid Suspension Flow Using a Laser-Anemometer System," *J. Phys. D.: Appl. Phys.*, **7**, 2288 (1974).

Beard, K. V., and H. R. Pruppacher, "A Determination of the Terminal Velocity and Drag of Small Water Drops by Means of a Wind Tunnel," *J. Atmos, Sc.*, **26**, 1066 (1969).

Boulos, M. I., and W. H. Gauvin, "Powder Processing in a Plasma Jet: a Proposed Model," *Can. J. Chem. Eng.*, **52**, 355 (1974).

Champagne, F. H., and I. J. Wygnanski, "An Experimental Investigation of Co-axial Turbulent Jets," *Int. J. Heat Mass Transfer*, **14**, 1445 (1971).

Durao, D. F. G., and J. H. Whitelaw, "Performance Characteristics of the Frequency Tracking Demodulators and a Counting System," Proc. of 2nd Int. Workshop on Laser Velocimetry, Purdue University, **1**, 170 (1974).

Durst, F., and H. Umhauer, "Local Measurements of Particle Velocities, Size Distribution and Concentration with a Combined Laser-Doppler Particle Sizing System," Proc. of LDA-75 Symposium, Technical University of Denmark (1975).

Durst, F., A. Melling, and J. H. Whitelaw, *Principles and Practice of Laser-Doppler Anemometry*, Academic Press, NY (1976).

Durst, F., "Studies of Particle Motion by Laser Techniques," Dynamic Flow Conference, Marseille (Sept., 1978).

Farmer, W. M., "Measurement of Particle Size and Concentrations Using LDV Techniques," Dynamic Flow Conference, Marseille (Sept., 1978).

Fiszdon, J., and J. Lesinski, "Accélération et Fusion des Grains dans un Jet de Plasma d'Argon-Hydrogène," International Roundtable on Study and Applications of Transport Phenomena in Thermal Plasmas, Odeillo (Sept. 12-16, 1975).

Gouesbet, G., and M. Trinite, "Anemometrie Doppler-Laser Haute Puissance dans un Jet de Plasma," Letters in Heat and Mass Transfer, **4**, 141 (1977).

Hamielec, A. E., T. W. Hoffman, and L. L. Ross, "Numerical Solution of the Navier-Stokes Equations for Flow Past Spheres," *AIChE J.*, **13**, 212 (1967).

Hinze, J. O., *Turbulence*, McGraw Hill Book Co., NY, 2nd ed., 534 (1975).

Lesinski, J., B. Mizera-Lesinska, J. C. Fanton, and M. I. Boulos, "LDA measurements under plasma conditions," 4th International Symposium on Plasma Chemistry, Zurich (Aug. 27-Sept. 1, 1979).

Lewis, J. A., and W. H. Gauvin, "Measurement of the Velocity of Particles Emerging from a Plasma Flame by High-Speed Cine-Streak

Photography," *J. Soc. Motion Picture Television Eng.*, **80**, 951 (1971).
Perry, M. G., and M. F. Handley, "The Dynamic Arch in Free Flowing Granular Material Discharging from a Model Hopper," *Trans. Ins. Chem. Eng.*, **45**, 367 (1967).
Reddy, K. VS., M. C. Van Wijk, and D. C. T. Pei, "Stereophoto-Grammetry in Particle-Flow Investigation," *Can. J. Chem. Eng.*, **47**, 85 (1969).
Richards, Bryan E., ed., *Measurement of Unsteady Fluid Dynamic Phenomena*, Hemisphere Publishing Corp. (1977).
Schichtin, H., *Boundary Layer Theory*, McGraw Hill Book Co., NY, 6th ed., 106 (1968).
Self, S. A., and J. H. Whitelaw, "Laser Anemometry for Combustion Research," *Combustion Sci. and Tech.*, **13**, 171 (1976).
Soo, S. L., *Fluid Dynamics of Multiphase Systems*, Blaisdell Publishing Co. (1967).
Stümke, A., and H. Umhauer, "Local Particle Velocity Distributions in Two-Phase Flows Measured by Laser-Doppler Velocimetry," Dynamic Flow Conference, Marseille (Sept., 1978).
Vardelle, A., M. Vardelle, J. M. Baronnet, and P. Fauchais, "Particles Velocity and Temperature Statistical Measurements in a d.c. Plasma Jet," 4th International Symposium on Plasma Chemistry, Zürich (Aug. 27-Sept. 1, 1979).

Manuscript received March 3, 1980; revision received July 17, and accepted July 25, 1980.

Drag Force Measurement of Single Spherical Collectors with Deposited Particles

HEMANT PENDSE
CHI TIEN
and
R. M. TURIAN

Department of Chemical Engineering and Materials Science
Syracuse University, Syracuse, New York 13210

The hydrodynamic drag force in a uniform flow field acting on a spherical body with small particles attached to its surface was determined experimentally. The experimental data are used to substantiate the approximate force expressions derived from available theories for several types of collector-particle geometries. Procedures for applying these results to the prediction of the pressure drop across a filter bed with various degrees of particle deposition are also developed.

SCOPE

Determination of the drag force acting on a spherical body with a number of smaller spheres attached to it is a very important problem in hydrodynamics, and because of its inherent complexity, it has been the subject of a number of investigations in the past. The purpose of this work was to examine the body of available results relating to this flow, to evaluate in detail their efficacy as practical means for predicting the drag force (i.e., over and above their representations as formal approximate mathematical solutions), to devise effective computational procedures appropriate to each, and to generate experimental data capable of providing critical tests of these results. The ultimate result of these tests was to develop accurate, yet relatively simple, procedures for estimating the drag force for creeping flow past such groups of spheres.

CONCLUSIONS AND SIGNIFICANCE

The drag force acting on a spherical body with a number of smaller spheres attached to it is basic to understanding deep bed filtration. The results of previous works have indicated the relevance of this flow to deep bed filtration, particularly in regard to determining the increase in pressure drop as the filter becomes progressively clogged. Principally, previous work has demonstrated that idealizing the filter grain by an equivalent spherical collector provided a convenient, yet sufficiently realistic, representation of the overall filtration process. In addition, calculations have indicated that the process of particle deposition within the filter progressed according to three main stages: a particle to grain deposition phase, followed by a dendritic growth phase, and concluding with a phase in which the deposition process is dominated by the consequences of interaction among dendrites. The significance of calculations of the drag forces for various configurations of sphere groupings corresponding to these stages of filtration is therefore evident, since they form the basis for predicting the relationship between the pressure drop across the filter with the degree of particle deposition.

R. M. Turian is presently with the Department of Energy Engineering, University of Illinois at Chicago Circle, Chicago, Illinois 60680. H. Pendse is with the Department of Chemical Engineering, University of Maine, Orono, Maine 04473.